PROCEEDINGS, 48th Workshop on Geothermal Reservoir Engineering
Stanford University, Stanford, California, February 6-8, 2023
SGP-TR-224

Model-Independent, and Model-Dependent Aspects of 'Geothermal Solute' Co-Production Forecast for Hydrothermal vs. Petrothermal Reservoirs

Julia Ghergut, Bettina Wiegand, Horst Behrens, Martin Sauter

Applied Geoscience Dept., Goldschmidtstr. 3, University of Göttingen, 37077, Germany

iulia.ghergut@geo.uni-goettingen.de

Keywords: geothermal lithium, solute mining, depletion, lifetime, fluid turnover, fluid residence time, inter-well, tracer test, artificial tracer, Upper Rhine Rift Valley, Oberrheingraben

ABSTRACT

We examine some model-independent, and model-dependent aspects of tracer-test inversion in the context of solute co-production from geothermal reservoirs, and explain two generic (model-independent) differences between solute depletion rates in petrothermal versus hydrothermal reservoirs, with major implications for the economic efficiency of any 'fluid mining' endeavor (for any solute species subject to 'geothermal co-production').

For geothermal systems operated by production/re-injection wells, 'thermal lifetime' is usually defined in terms of a temperature drop threshold, and estimated as a function of fluid turnover time (or mean residence time MRT) and heat exchange surface-area-per-volume (σ), with MRT hopefully measurable by means of a tracer test, whereas σ is rather difficult to infer from tracer signals alone. Deriving MRT from measured artificial-tracer signals looks (formally) model-independent, but is subject to large-time extrapolation uncertainty (which restores model dependence).

Following the analogy between 'thermal drawdown' and solute depletion, a 'solute co-production lifetime' may also be defined. Unlike for thermal predictions, however, tracer-based conservative estimations of (cumulatively co-produced) solute output (viz., of its lower-bound level, assuming conservative transport by fluid turnover only, non-replenished from adjacent rock) are much less impeded by MRT uncertainty, but essentially depend on the maximum (asymptotic large-time) recovery ratio R_{max} (%) of the injected artificial tracer (which, again, restores model dependency, but w. r. to structural features that are much less relevant for thermal predictions). Once a tracer test was conducted in accordance with the rules of the art, the reservoir can be treated like a black box with a response function derivable, in a well-defined manner, from the artificial-tracer signal (as long as the flow regime does not change significantly). The gradual solute depletion can be described by a dimensionless 'time deficit' term $\tau - \mu(\tau)$. A tracer signal 'type curve' approach, with decreasing Péclet number (Pe) in guise of increasing georeservoir heterogeneity (or increasing 'petrothermal character'), reveals how early solute output rates falsely suggest too low a value for $\tau - \mu(\tau)$, thereby considerably over-estimating the total extractable mass and prompting excessively optimistic expectations. The error, though, decreases with decreasing Pe. Type-curve comparison shows solute co-production proceeds more efficiently in homogeneous, than in heterogeneous flow fields of same MRT. By the same token, co-production efficiency ought to be higher in hydrothermal, than in petrothermal reservoirs of same MRT (moreover, petrothermal system 'engineering' to date fails to reach MRT sizes comparable to those of hydrothermal systems), whereas hydrothermal systems are more prone to over-optimistic mispredictions of cumulative solute output.

Besides the generic, model-independent tracer-based forecast framework (with type-curve extensions, after re-normalizing the double-convolution integral that was derived by Behrens et al 2022), the model-dependent use of early ('undetectable') signal 'information' to infer lower bounds on "geothermal lithium" output is illustrated for a tracer test presently initiated in the Upper Rhine Rift Valley, already indicating a mass output of several thousand tons over the next three decades.

1. INTRODUCTION

What do we need to know about a geothermal well doublet, besides inter-well tracer signals, to enable predicting thermal drawdown and, where applicable, solute co-production output? And why are we addressing the latter – for lithium in particular? In continental Europe, dissolved lithium levels in georeservoir fluids below ~3 km depth look promising (~150 to 250 mg/L, Feldbusch 2016, Sanjuan et al. 2020, 2022; cf. also Kühn et al. 1998, 2002; Eggeling et al. 2013, Stober et al. 2013, Stober and Bucher 2015, Kölbel et al. 2020, Drüppel et al. 2020, Frey et al. 2022, Herzberger alias Orywall et al. 2009, 2010) at various sites in the Upper Rhine Rift Valley (URRV) and the N-German Basin (NGB), and Li extraction seems attractive for a number of reasons: the assumed rise in market demand, while at the same time aiming to curb the environmental footprint of Li mining – which co-production within a geothermal-well doublet can manage thanks to its closed fluid loop; last but not least, making the economic efficiency gap of geothermal itself look less dramatic.

In the typical geothermal reservoir, operated by a well doublet loop, continuously re-injecting a 'spent fluid' that is colder than the initial (undisturbed) reservoir is going to gradually cool the reservoir. The cooling front is hopefully slower than the fluid's advection, by a (more or less constant) factor we would like to be able to predict before it has reached the production well, i. e. well in advance of a thermal drawdown becoming detectable at the production well. This will happen slower or faster, depending on (site-specific)

georeservoir properties – which implies some kind of model dependence. Similarly, with solute co-production, continuously re-injecting a fluid which is depleted in the particular constituent(s) we have removed from it (by our uphole extraction technology) before re-injection, will gradually deplete the entire circulation loop, and this is going to occur faster than the thermal drawdown. We can define a 'solute co-production lifetime', complementary to 'thermal lifetime'; we endeavor to infer both from (artificial-)tracer test signals, which are supposed to become detectable well in advance – in order to avoid misinvestment, since the sizing design and running costs of solute extraction and (on-site or logistically site-contiguous) processing facilities are substantial.

In terms of thermal drawdown, we know that the reservoir size is primarily measured by fluid residence times – but not only by them. Especially for fractured reservoirs, we need to additionally quantify features like a heat exchange surface area (per flow volume), or an equivalent fracture spacing, in multiple-fracture systems. In any case, the relationship between thermal drawdown and fluid (mean) residence times (M)RT, as 'measurable' by tracer tests, remains essentially parametric, and it contains some crucial parameters which tracer tests alone cannot quantify unambiguously; the reservoir type (hydro- or petrothermal) also matters. Deriving MRT from artificial-tracer signals looks model-independent (formally), but is subject to large-time extrapolation uncertainty, which may restore model-dependence. By contrast, the solute co-production lifetime relates to the tracer signal (which is equivalent to the fluid's residence time distribution, RTD) in an essentially *non-parametric* way: solute mass output as a function of time is merely an integral transform on the measured tracer signal (whose RTD can be regarded as a Green's function surrogate for the mass transport problem), further allowing for scaled (dimensionless) considerations, regardless of reservoir size and type, and reducing to even simpler transforms when the fluid turnover rate Q is constant. In the sequel, notations TOV or V_{fluid}, MRT or T_{fluid} are used interchangeably for the reservoir's turnover volume and the fluid's mean residence time in it, under a given flow regime with flow rate Q; the former wording is more common in the geothermal community, whereas the latter renders formal similarities of fluid / solute / heat transport easier to recognize.

2. TRACER-BASED FORECAST APPROACH

Behrens et al. (2022) presented a tracer-based method to forecast the depletion of a co-produced solute during fluid turnover, and illustrated its use for various reservoir settings, with a special focus on Soultz-sous-Forêts in the URRV and Horstberg in the NGB. The method is model-independent, viz. the measured signals of any conservative artificial tracer, from inter-well or single-well circulation tests conducted under representative flow conditions, can be used to predict the future co-production output of any fluid-mined solute (in particular: lithium), and its gradual depletion during fluid turnover, regardless of the availability and parametrizing of a reservoir model (distributed- or lumped-parameter, numerical or analytical).

We first recall relationships (3) – (5) from Behrens et al. (2022) concerning 'thermal lifetime' definition and major parameters' contrast (magnitude-order disparities) for petrothermal (PT) vs. hydrothermal (HT) reservoirs. – By the same token, we can define a "solute co-production lifetime" T_{sol} which, in the absence of solute replenishment processes, obviously equals the fluid residence time, $T_{sol} = T_{fluid}$; thus $T_{sol} < T_{heat}$ always. Defining $\theta = T_{sol} / T_{heat}$, the share of the reservoir's total (thermal) lifetime required to reach a solute depletion plateau, θ values for petro- and hydrothermal reservoirs of similar size (same MRT = TOV /Q) compare to each other like (factors R, D, σ were defined in Behrens et al. 2022)

$$\theta_{PT} / \theta_{HT} = R_{HT} / (D_{PT} \sigma_{PT}^2 \; T_{fluid}) ,$$

the numerator being (significantly) larger than 1, whereas the denominator is supposed to be very much larger than 1, implying solute co-production efficiency ought to be higher in PT, than in same-size HT reservoirs; if real-world reservoirs tell a different story, it is because

► reality is hostile: falling short of PT reservoir development or 'engineering', regardless of solute extraction effectiveness

► our "θ" model is too simplistic: discarding non-advective transport in the reservoir (which plays the essential part in PT systems!)

Unlike for thermal predictions, however, tracer-based conservative estimations of (cumulatively co-produced) solute output (viz., of its lower-bound level, assuming conservative transport by fluid turnover only, non-replenished from adjacent rock) are much less impeded by MRT and transport process quantification uncertainty, but essentially depend on the maximum (asymptotic large-time) recovery ratio R_{max} (%) of the injected artificial tracer (which, again, restores model dependency, but w. r. to structural features that are much less relevant for thermal predictions). The conservative forecast of co-produced solute mass output as a function of time, as resulting from a mixing relationship (Behrens et al., 2022) between the undisturbed-reservoir fluid with solute concentration C_{ini} and the re-injected fluid with usually non-zero 'residual' concentration C_{resid},

$$M_{out}(t) \;=\; (C_{ini} - C_{resid}) \; [\, VOL_{out}(t) - \int_o^t \int_o^{t'} Q(t') \, Q(t'') \, g(t'') \, dt'' \, dt' \,]$$

requires just knowledge of conservative-tracer fluxes within the forecasting time horizon. Once a tracer test was conducted in accordance with the rules of the art (which includes approximate observance of well-defined, usually flux-type boundary conditions for fluid sampling and for tracer input, cf. Kreft and Zuber, 1978), the reservoir can be treated like a 'black box' with 'response function' (Green's kernel surrogate) g.

3. SCALING CONSIDERATIONS

If solute 'replenishment' (say, by ion exchange or de-sorption processes) from adjacent rock remains negligible, the solute contents of the mobile-fluid TOV ($V_{fluid} = Q\,T_{fluid}$, when Q is steady) yields an upper bound on the maximum extractable solute mass (whereas the maximum amount of the latter can stay well below the former, for the chosen duration of reservoir operation). Normalizing the cumulatively co-produced solute mass M_{out} by this upper bound, we get

$$[\,(C_{ini}–C_{resid})\,V_{fluid}\,]^{-1}\;M_{out}(\tau) \;\equiv\; \mu(\tau) \;=\; \tau - \int_0^{\tau} \eta(\tau')\,d\tau'$$

as a function of dimensionless time $\tau \equiv t / T_{fluid}$, where η denotes the cumulative tracer recovery, normalized by the tracer input mass, and expressed as a function of dimensionless time τ. Thus, at early times ($t << T_{fluid}$), the extracted mass fraction grows proportionally with time, scaled 1:1 like τ; with physical units, the early growth rate equals $Q\,(C_{ini}–C_{resid})$. Extrapolating this early growth rate to later times would tremendously over-estimate M_{out} , because the growth rate drops significantly below 1 in scaled terms ($\mu < \tau$) when $t > T_{fluid}$.

Such solute depletion behavior was analyzed in more detail by Behrens et al. (2022), based on actual tracer signal data from past tests, for the pilot-geothermal site Horstberg in the NGB (Ghergut et al., 2016), and for Soultz-sous-Forêts in the URRV (using data from Blumenthal 2007), showing that the asymptotic mass output is less than one third of what early extraction rates would have 'predicted'. Here, a broader view is achieved in dimensionless 'type curve' format, enabling to compare between reservoirs of different sizes (in terms of their TOV and/or MRT) , operated at different rates, by assuming a single Péclet number can roughly quantify heterogeneity at reservoir scale, $Pe \equiv V_{fluid} / (S\,\alpha_{longit})$ with S the average cross-section area available for fluid flow, and α_{longit} the relevant 'longitudinal dispersivity' for the given flow regime. The stronger the heterogeneity, the lower the Pe number; for uniform (piston-like) flow, $Pe \to \infty$. Whereas the advective-dispersive model for conservative solute transport would forbid Pe values lower than 1, one may use fictional values "$Pe \leq 1$" to roughly reproduce some 'matrix diffusion' effects (which are not included with the advective-dispersive model, but are likely to play a most significant part in tracer transport through the consolidated-rock formations of the deeper subsurface). Roughly speaking, the lower the Pe value, the more pronounced the 'fractured' or 'petrothermal' character of the reservoir – irrespective of its geological classification as 'sedimentary' rather than 'crystalline'. Allowing Pe to span three orders of magnitude (from 100 to $1/\sqrt{10}$), we obtain the normalized tracer signal and cumulative recovery 'type curves' of fig. 1, with flow-storage distribution (FSD) patterns shown beneath, along with FSD derived from actual tracer-test data (cf. supra) of what we may now deem 'petrothermaquifers' (reservoirs of hybrid complexion, more 'petrothermal'-like in he NGB, more 'hydrothermal-like' in the URRV). Shook (2003) was the first to propose FSD for geothermal system analysis; a slightly transformed FSD kind (Behrens et al. 2010) enhances the visibility of equivalent 'matrix diffusion' effects on conservative solute transport; additionally, the magnitude of immobile-fluid compartment effects is best recognized in logarithmic scaling. For the tracer signals (type curves) of fig. 1, the normalized-time deficit amount $\tau - \mu(\tau)$ (cf. supra) grows with time as shown beneath; these deficit values are then used to predict the receding $\mu(\tau)$ growth and co-extraction rates $\mu(\tau) / \tau$ as shown in fig. 2, in whose ordinate-axis labels ΔC abbreviates the solute concentration difference $C_{ini}–C_{resid}$ (for the co-produced solute only, not for the artificial tracer), with C_{resid} assumed as constant for simplicity (C_{resid} is a technical parameter of the solute extraction technology, say, by means of ion exchange, as implemented in some uphole facility; C_{resid} will depend on column sizes used, retention times, etc.; it is essentially unrelated to solute transport processes within the georeservoir flow field).

To be noted, in order to define a Green's function surrogate g , the measured tracer signal needs to be properly normalized by its total, i. e. asymptotic large-time recovery R_{max} (%), and in order to estimate the latter a reservoir model might still be needed – especially, one needs to know how 'tight' or 'open' its remote boundaries are (which the tracer hasn't "seen" yet, so to say, and which might significantly contribute to solute replenishment, adding to the solute co-production output, cf. fig. 4).

4. 'UNDETECTABLE SIGNAL' OF ARTIFICIAL TRACER YIELDS MODEL-DEPENDENT ESTIMATES OF LOWER BOUNDS ON CUMULATIVE SOLUTE OUTPUT

At early stages of artificial-tracer signal monitoring, we can attempt to estimate a lower bound on MRT based on knowledge that the signal stays below detection limit DL until at least a certain time t_1 . This can be achieved by comparing the hyperbolae of scaled detection limit $\varepsilon(\tau) = (DL\,Q\,t_1) / (R_{max}\,M_{tracer\,input}\,\tau)$, as a function of scaled time τ , with the ascending interval of scaled signal type-curves like those of figure 1. This approach is model-dependent, because we need to make assumptions about the transport processes (like advection – dispersion "only", as for fig. 1), as well as about reservoir structure, especially its boundaries and flow-field convergence/divergence at reservoir scale, which determines the asymptotic tracer recovery ratio $\eta(\tau\to\infty) = R_{max}$. This early-stage 'inverse problem' or 'parameter identification' job is illustrated in fig. 5 for an URRV (supposedly hydrothermal) reservoir, whose 'fingerprint' values of Q , $M_{tracer\,input}$, DL and t_1 cannot be disclosed due to commercial implications – but its MRT estimates derived for 2 x 2 limiting values of Pe and R_{max} are shown in figs. 5 – 6 along with their corresponding "geothermal lithium" output predictions; here, 'limiting' means: Pe higher than 30 or below 1 are regarded as implausible, and R_{max} less than 10% or more than 60% seem very unlikely; these are just two different aspects of 'model dependence'. For the advective-dispersive model, t*/MRT can be tabulated as a function of Pe and R_{max} .

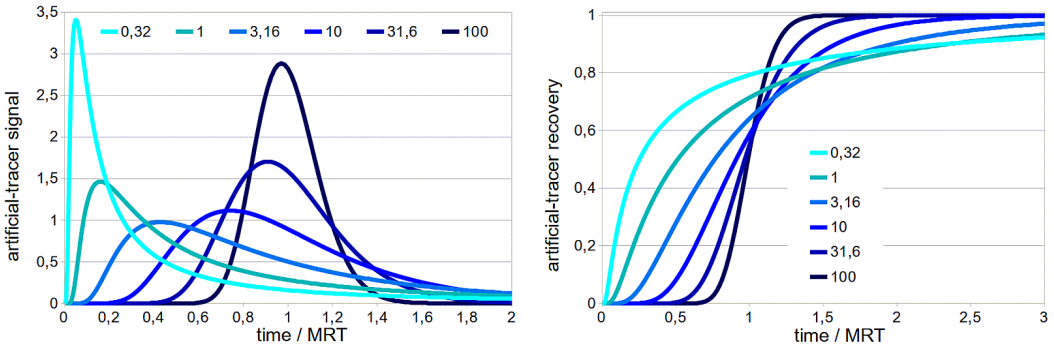

type curves : normalized tracer signals and their cumulative recovery ratio, with Pe between 100 and $1/\sqrt{10}$

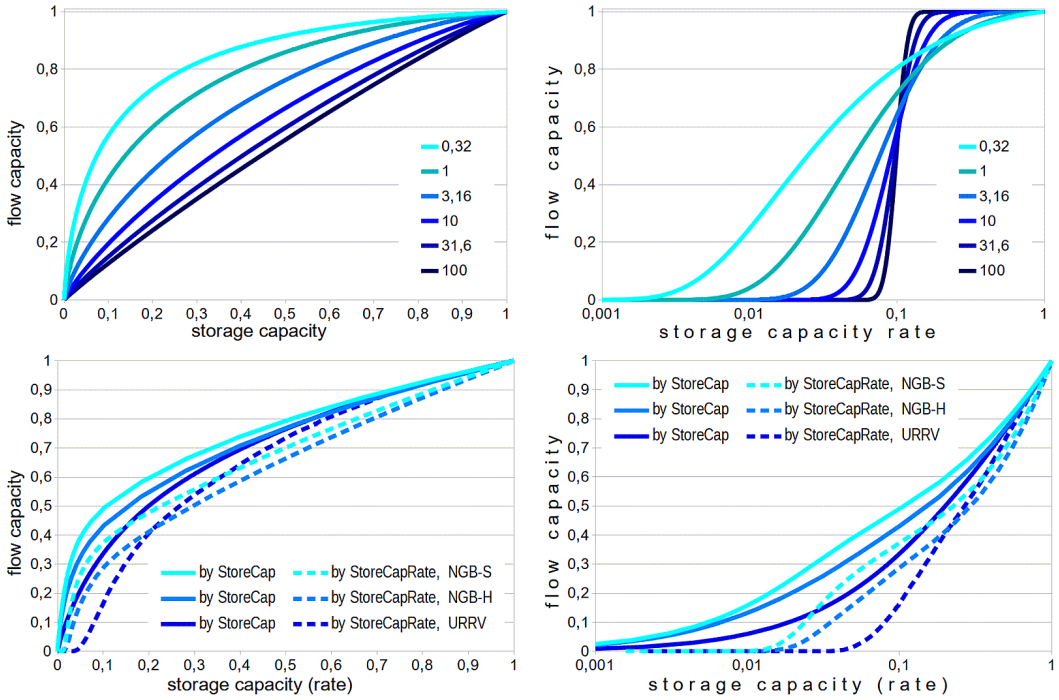

flow-storage distribution associated to the same Pe values ; for comparison, the lower row shows FSD derived from tracer-test data obtained for geothermal reservoirs of hybrid complexion ('petrothermaquifer') in the NGB and the URRV (after Behrens et al. 2022). The modified FSD plot (by storage capacity rate) enhances the visibility of equivalent 'matrix diffusion' effects on conservative solute transport; immobile-fluid compartment best recognized in logarithmic scaling.

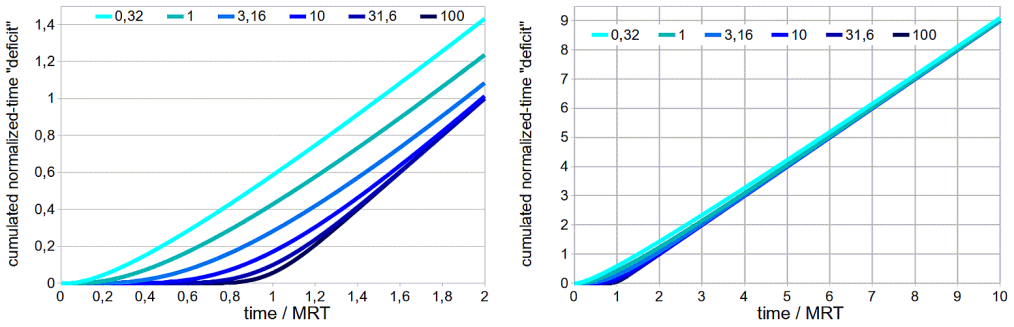

cumulative dimensionless-time deficit μ(τ) for the same Pe values ; the early Pe sensitivity vanishes at later stages

Figure 1: Workflow of the type-curve approach described in section 3, deriving the 'time deficit' term for systems with varying degree of heterogeneity.

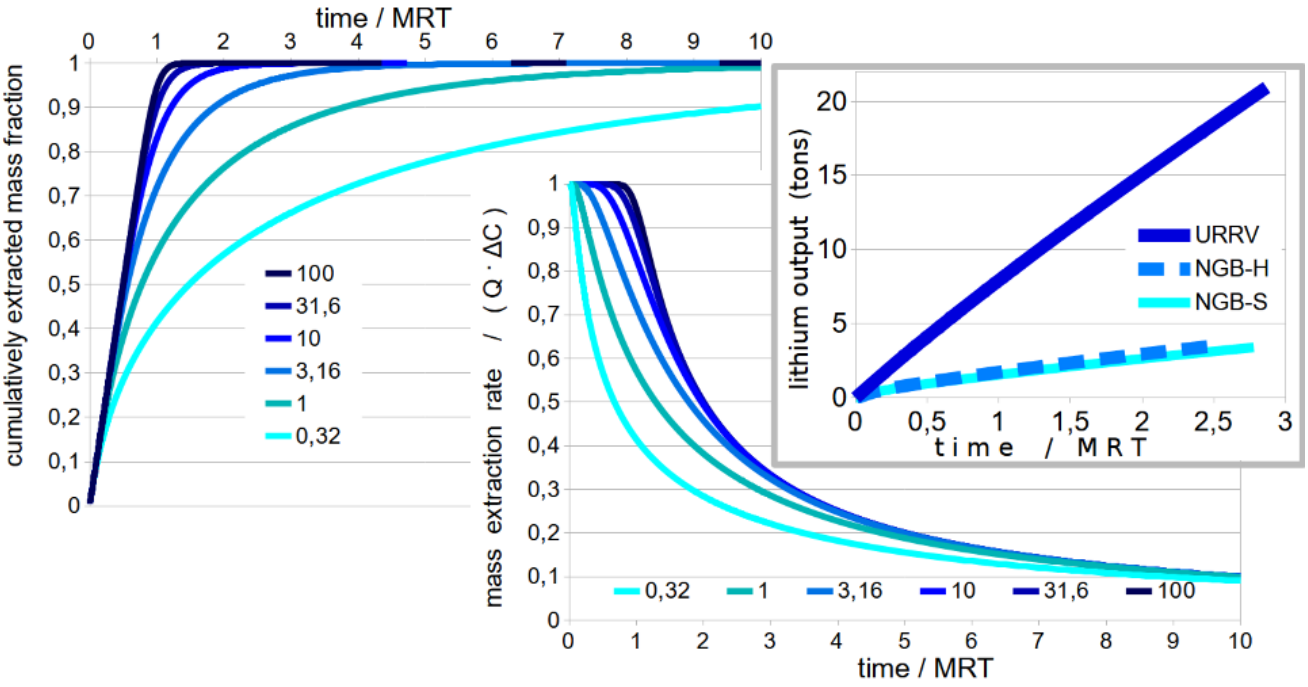

Figure 2: Co-produced solute mass output, and mass extraction rate drop corresponding to the Pe values (type curves) of fig. 1; for comparison, the insert shows the tracer-based prediction of early lithium output for the geothermal reservoirs in the URRV and the NGB, whose flow-storage distribution was shown in the third row of fig. 1.

Figure 3: The findings from state-of-the-art laboratory-instrumental analytics on fluid samples, no less than the performance of tracer technologies in real-world reservoirs, rarely match the clear-cut expectations from type-curve families …

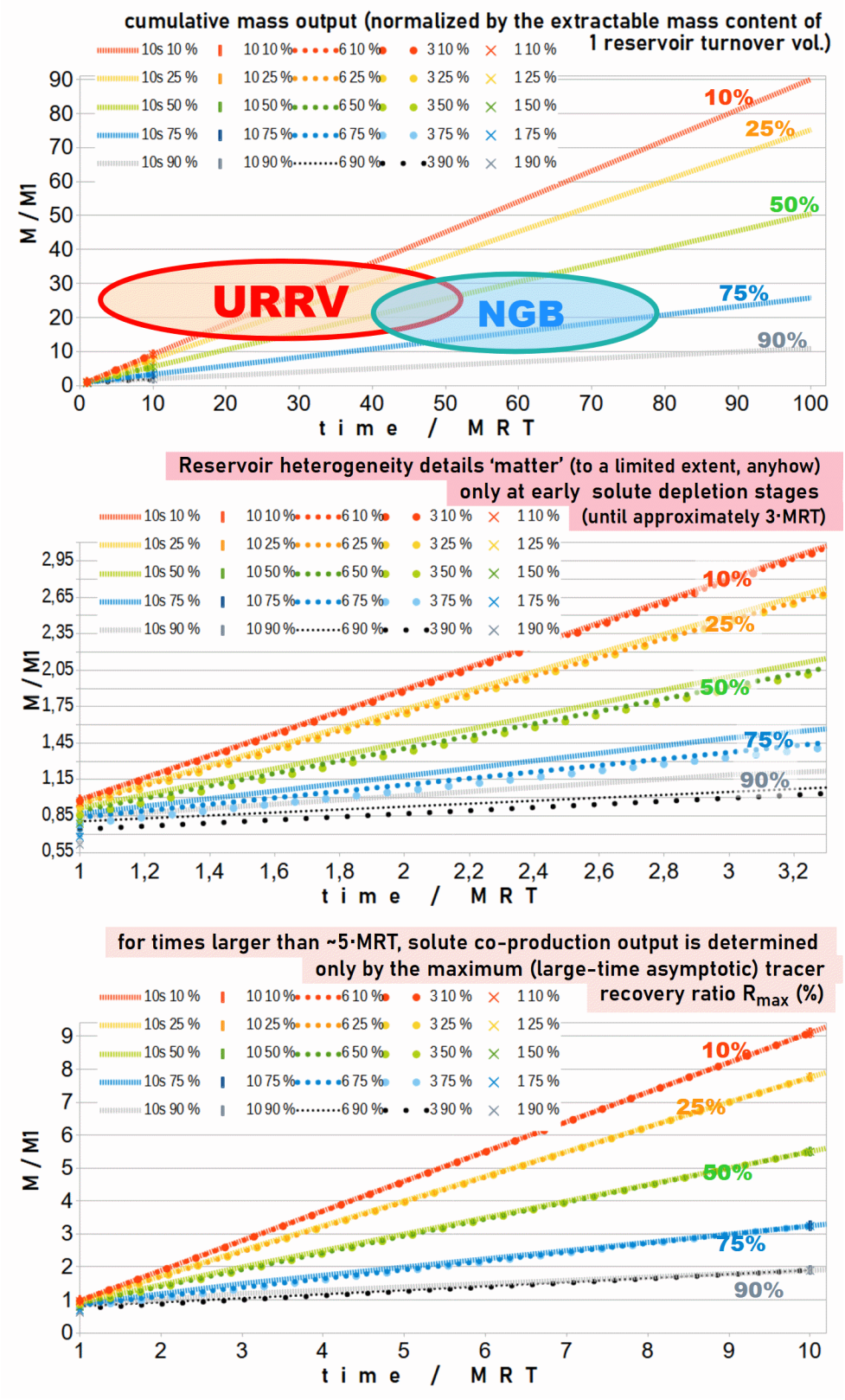

Figure 4: Mid-term to long-run, conservative 'fluid mining' output forecast is controlled solely by R_{max} (%), regardless of further reservoir details.

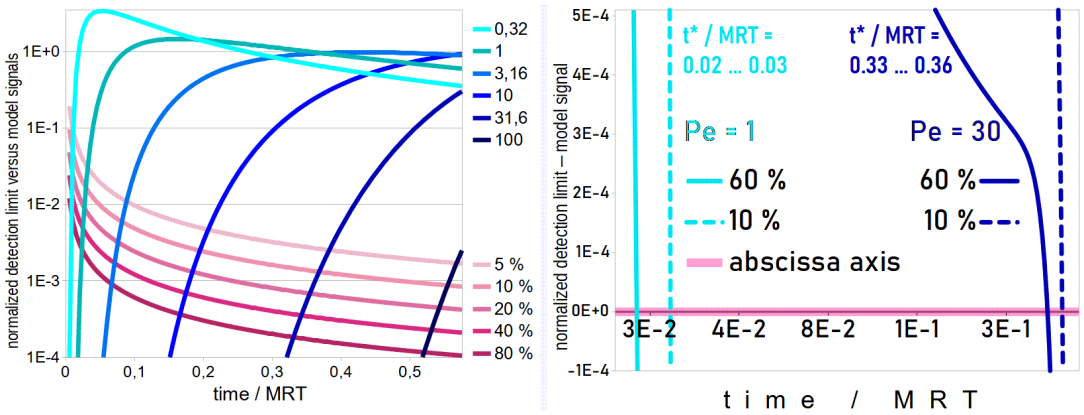

Figure 5: Workflow for inferring MRT from 'nil signal' information, assuming some contrasting Pe and R_{max} (%) values.

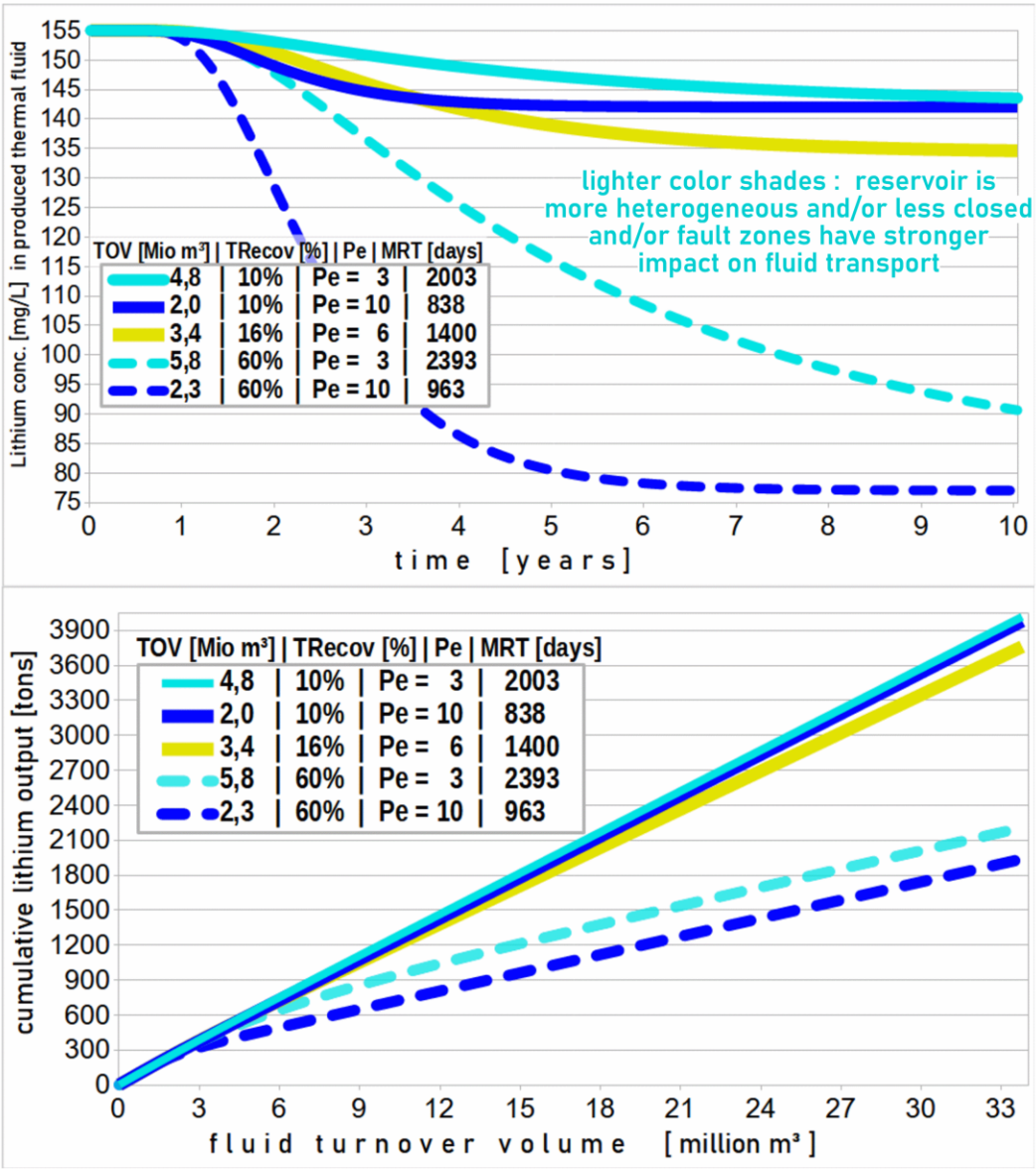

Figure 6: Lithium output forecast derived from MRT 'solutions' obtained numerically (using Mathematica's NSolve) or graphically from figure 3, with prescribed values for R_{max} (%) and Pe.

In the l.-h.s. of fig. 5, the hyperbolae of normalized DL versus scaled time (in violet shades) intersect a type-curve family of normalized tracer signals (in blue shades). The former is model-dependent in terms of the assumed value for R_{max} (%), which primarily reflects reservoir boundaries and flow-field divergence/convergence at reservoir scale. The type-curve family is independent of R_{max} (%), being already normalized by it, but is constrained by the assumption of unimodal (single Pe value for) advective-dispersive transport of the conservative tracer between injection and production well. The r.-h. s. diagram of fig. 5 illustrates the non-unique 'inversion' (numerical solution of transcendental equation) of a fluid MRT value from the abscissa intersection of the difference (violet – blue) curve family in the range comprised between two contrasting values for R_{max} (60% for 'rather closed', 10% for 'rather open' reservoir) and two contrasting values for Pe (dark blue: Pe = 30 for 'very homogeneous'; light blue: Pe = 1 standing for 'very heterogeneous' reservoir).

4. CONCLUDING REMARKS

Early solute output rates falsely suggest too low a value for the 'time deficit' term. Extrapolating early ($\tau - \mu(\tau)$) trends to later stages would tremendously overestimate the total extractable mass, prompting excessively optimistic expectations. As can be recognized from the l.-h. s. of fig. 2, the higher the Pe value (i. e., the more homogeneous the reservoir), the greater the exaggeration of forecast over-optimism. This might explain the somewhat dramatic contention the geothermal community has recently witnessed concerning a particular site in the URRV: the early solute co-production data have been reported correctly, but their late-time extrapolation was unreliable. Interestingly, ($\tau - \mu(\tau)$)'s dependence on Pe (i. e., on reservoir heterogeneity, or on its 'occult petrothermal' character) seems to vanish (fig. 1, last row) with increasing time; notwithstanding, co-produced solute output as well as production rates (fig. 2, fig. 6) still show a sensible dependence on Pe, most strikingly for the curves in light cyan, corresponding to "Pe < 1" which actually means violating the advective-dispersive model and forcibly bringing in matrix diffusion; the curves in sea-foam green (Pe = 1) delineate between advective-dispersive and 'matrix-diffusive' regimes of solute transport. Roughly speaking, the stronger the heterogeneity or permeability contrast a.k.a. discontinuity (or 'petrothermal') features, the longer it would take (in terms of normalized time) to 'pull' the maximum-possible solute contents 'out' of the reservoir. Conversely, the more homogeneous the reservoir, the more efficient the solute co-production. This is the take-away message from such simplistic type-curve calculations.

Further non-trivial challenges result from the need to foresee and quantify overall water-rock interaction effects of 'spent fluid' re-injection, the latter being depleted of its particular micro-constituent, albeit at trace levels only, while being likely acidized or 'unreliably' buffered at major-ion levels. Water-rock interactions cannot be told from conservative-tracer signals; hydrogeochemical modeling (Kühn et al. 2002, Maier et al. 2021) becomes indispensable and is likely to turn out more intricate for hybrid 'petrotherm-aquifers' in the NGB (Kühn et al. 1998, Tischner et al. 2010, Feldbusch 2016) than for hydrothermal reservoirs in the URRV (Kölbel et al. 2020).

The co-operative research project UnLimiteD (www.geothermal-lithium.org/en), initiated by EnBW (Energie Baden-Württemberg) together with BESTEC (www.bestec-for-nature.com), KIT (Karlsruhe Institute of Technology) and the University of Göttingen, deals with lithium co-production from geothermal reservoirs in the URRV and the NGB. The Göttingen working group uses fluid tracers, natural and artificial, to estimate the overall lithium amount extractable by fluid mining in various geological settings, quantify the evolution of solute co-production rates during fluid turnover, and predict the final mass and energy output over the solute mining lifetime (which may or not exceed the thermal lifetime of a given reservoir, depending on its operation schemes). Complementarily to the *model-independent* approach of Behrens et al. (2022), we currently rely on the incipient (nil) signal from the inter-well tracer test which started in late February 2022 at a geothermal well doublet on the German side of URRV, to estimate lower-bounds on fluid residence times and reservoir turnover volume. Knowing that the tracer signal at the production well stays below a specified detection limit for a duration of at least t_{nil} since the tracer was added at the re-injection well, thereby derived values for RT and TOV are then used to predict lithium depletion and the total lithium output expectable over the reservoir lifetime. This approach, however, is *model-dependent* in that it relies on certain assumptions on reservoir structure and boundaries constraining the large-time asymptotic tracer recovery R_{max} (%). Lowering the DL level (due to progress in laboratory-instrumental capabilities beyond state-of-the-art) from 0.2 ppb to 20 ppt for all fluid samples collected during the same t_{nil} (~6 months) raises the predicted lithium output from 3.9 to 4.3 kilotons for the first three decades. – not a spectacular 'increment', but it keeps increasing (non-linearly) as t_{nil} increases, and the latter can indeed be expected (based on structural-model considerations, cf. Meixner 2009, Meixner et al. 2016) to increase significantly (in the order of years), regardless of DL improvement.

5. ACKNOWLEDGMENTS

We gratefully acknowledge invaluable operational support from Julia Scheiber, Thomas Hettkamp and their BESTEC team, from Elif Kaymakci, Thomas Kölbel and their EnBW team, fruitful cooperation with Lena Kölbel and her HYDROSION team, last but not least with the Applied Geology chair along with the Geothermics working group at the University of Karlsruhe, led by Heinz Hötzl, Leif Wolf, Detlev Rettenmaier and Jörg Meixner, as well as long-term financial support from Germany's Federal Ministry for Economic Affairs and Energy (BMWi projects "LOGRO" and "UnLimiteD" under grant nos. / FKZ 0325111B, 03EE4023E).

REFERENCES

Behrens, H., Ghergut, J., Sauter, M., Wagner, B., Wiegand, B.: Solute co-production from small geothermal reservoirs – how little is too little?, Proceedings, 47th Workshop on Geothermal Reservoir Engineering, Stanford University, Stanford, CA (2022), SGP-TR-223, 200–210.

Behrens, H., Ghergut, J., Sauter, M.: Tracer properties, and tracer test results – part 3: modification to Shook's FSD method, Proceedings, 35th Workshop on Geothermal Reservoir Engineering, Stanford University, Stanford, CA (2010), SGP-TR-188.

Blumenthal, M.: Numerische Modellierung hydraulischer und thermischer Prozesse im tiefen Wärmereservoir bei Soultz-sous-Forêts, Frankreich, Diplomarbeit (university graduation thesis, equiv. to M. Sc. thesis), RWTH University of Aachen, Germany (2007).

Drüppel, K., Stober, I., Grimmer, J. C., Mertz-Kraus, R.: Experimental alteration of granitic rocks: Implications for the evolution of geothermal brines in the Upper Rhine Graben, Germany, Geothermics, 88 (2020), 101903.

Eggeling, L., Genter, A., Kölbel, T., Münch, W.: Impact of natural radionuclides on geothermal exploitation in the Upper Rhine Graben, Geothermics, 47 (2013), 80–88.

Feldbusch, E.: Geochemische Charakterisierung eines Formationsfluids im Unteren Perm: Herkunft, betriebsbedingte Prozesse und Rolle organischer Verbindungen im geothermischen Kreislauf, Ph.D. Thesis, Universität Potsdam (2016).

Frey, M., Bär, K., Stober, I., Reinecker, J., van der Vaart, J., Sass, I.: Assessment of deep geothermal research and development in the Upper Rhine Graben, Geothermal Energy, 10:18 (2022), doi 10.1186/s40517-022-00226-2

Ghergut, J., Behrens, H., Sauter, M.: Petrothermal and aquifer-based EGS in the Northern-German Sedimentary Basin, investigated by conservative tracers during single-well injection-flowback and production tests, Geothermics, 63 (2016), 225–241.

Herzberger, P., Kölbel, T., Münch, W.: Geothermal Resources in the German Basins, GRC Transactions, 33 (2009), 395–397.

Herzberger alias Orywall, P., Münch, W., Kölbel, T., Bruchmann, U., Schlagermann, P., Hötzl, H., Wolf, L., Rettenmaier, D., Steger, H., Zorn, R., Seibt, P., Möllmann, G.-U., Sauter, M., Ghergut, J., Ptak, T.: The Geothermal Power Plant Bruchsal, Proceedings, World Geothermal Congress (2010), paper 0619.

Kölbel, L., Kölbel, T., Maier, U., Sauter, M., Schäfer, T., Wiegand, B.: Water-rock interactions in the Bruchsal geothermal system by U-Th series radionuclides, GeoThermalEnergy (GTE), 8 (2020), 24.

Kreft, A., and Zuber, A.: On the physical meaning of the dispersion equation and its solutions for different initial and boundary conditions, Chem. Eng. Sci., 33 (1978), 1471–1480.

Kühn, M., Bartels, J., Pape, H., Schneider, W., Clauser, C.: Modeling chemical brine-rock interaction in geothermal reservoirs, In: Stober, I. and Bucher, K. (eds.), Water-Rock Interaction, Water Science and Technology Library, vol. 40 (2002), Springer, Dordrecht, doi 10.1007/978-94-010-0438-1_6

Kühn, M., Niewöhner, C., Isenbeck-Schröter, M., Schulz, H.D.: Determination of major and minor constituents in anoxic thermal brines of deep sandstone aquifers in Northern Germany, Water Research 32 (1998), 265–274, doi 10.1016/S0043-1354(97)00252-2

Maier, U., Tatomir, A., Sauter, M.: Hydrogeochemical modeling of mineral alterations following CO2 injection, Applied Geochemistry, 136 (2021), 10515.

Meixner, J.: Konzeptionelle hydrogeologische Modellansätze als Vorstudie für ein integriertes Standortmodell, Master's Thesis, Karlsruher Institute of Technology (Germany), KIT Diploma Theses / Archives (2009), Chapter 5.

Meixner, J., Schill, E., Grimmer, J. C., Gaucher, E., Kohl, T., Klingler, P.: Structural control of geothermal reservoirs in extensional tectonic settings: An example from the Upper Rhine Graben, J. Struct. Geol., 82 (2016), 1–15.

Sanjuan, B., Gourcerol, B., Millot, R., Rettenmaier, D., Jeandel, E., Rombaut, A.: Lithium-rich geothermal brines in Europe: An update about geochemical characteristics and implications for potential Li resources, Geothermics, 101 (2022), 102385.

Sanjuan, B., Negrel, G., Le Lous, M., Poulmarch, E., Gal, F., Damy, P.-C.: Main geochemical characteristics of the deep geothermal brine at Vendenheim (Alsace, France) with constraints on temperature and fluid circulation, Proceedings, World Geothermal Congress (2020=, Reykjavik, Iceland, paper 31005.

Shook, G. M.: A Simple, Fast Method of Estimating Fractured Reservoir Geometry from Tracer Tests, Geothermal Resources Council Transactions, 27 (2003), 407–411.

Tischner, T., Evers, H., Hauswirth, H., Jatho, R., Kosinowski, M., Sulzbacher, H.: New Concepts for Extracting Geothermal Energy from one Well: The GeneSys-Project, Proceedings, World Geothermal Congress, Bali, Indonesia (2010), paper 2272.

Stober, I., and Bucher, K.: Hydraulic and hydrochemical properties of deep sedimentary reservoirs of the Upper Rhine Graben, Europe, Geofluids, 15 (2015), 464–482.

Stober, I., Jodocy, M., Hintersberger, B.: Gegenüberstellung von Durchlässigkeiten aus verschiedenen Verfahren im tief liegenden